Korean J. Chem. Eng., 33(12), 3448-3455 (2016)
DOI: 10.1007/s11814-016-0185-4

pISSN: 0256-1115
eISSN: 1975-7220

Effects of alkali-metal carbonates and nitrates on the CO_2 sorption and regeneration of MgO-based sorbents at intermediate temperatures

Soo Chool Lee*,‡, Su Ho Cha,‡, Yong Mok Kwon***, Myung Gon Park***, Byung Wook Hwang***, Yong Ki Park****, Hwi Min Seo****, and Jae Chang Kim***,†**

*Research Institute of Advanced Energy Technology, Kyungpook National University, Daegu 41566, Korea
**Research & Development Division Energy Plant R&D Team, Hyundai Engineering & Construction Co., Ltd., Yongin-si 16891, Korea
***Department of Chemical Engineering, Kyungpook National University, Daegu 41566, Korea
****Green Chemistry Division, Korea Research Institute of Chemical Technology, Daejeon 34114, Korea
(*Received 1 March 2016 • accepted 28 June 2016*)

Abstract—The effects of alkali-metal carbonates and nitrates on the CO_2 sorption and regeneration of MgO-based sorbents were investigated in the presence of 10 vol% CO_2 and 10 vol% H_2O in an intermediate temperature range, 300 to 450 °C. The CO_2 capture capacities of the MgO-based sorbents promoted with Na_2CO_3 and K_2CO_3 were 9.7 and 45.0 mg CO_2/g sorbent, respectively. On the other hand, a MgO-based sorbent promoted with both Na_2CO_3 and $NaNO_3$ exhibited the highest CO_2 capture capacity of 97.4 mg CO_2/g sorbent at 200 °C in 10 vol% CO_2, which was almost ten-times greater than that of the MgO-based sorbent promoted with Na_2CO_3. The CO_2 sorption rate of these sorbents was higher than that of the MgO-based sorbents promoted with alkali-metal nitrates due to the formation of $Na_2Mg(CO_3)_2$ or $K_2Mg(CO_3)_2$ by the alkali-metal carbonate and the eutectic reaction of the alkali-metal nitrates. In addition, the reproducibility problem of double-salt sorbents obtained by the precipitation method was completely resolved by impregnating MgO with alkali-metal carbonates and nitrates. Furthermore, we found that their desorption temperatures are lower than those of the MgO-based sorbents promoted with alkali-metal carbonates due to the eutectic reaction during the regeneration process.

Keywords: Nitrate, MgO, CO_2, Capture, Intermediate Temperature, Molten Salt

INTRODUCTION

The amount of greenhouse gases emitted into the atmosphere has increased dramatically as a result of the increasing demand for fossil fuels due to industrialization [1,2]. The introduction of versatile carbon capture and storage (CCS) systems is currently the most attractive and practical solution to the greenhouse gas problem [3-6]. Among these, CO_2 capture processes using regenerable solid sorbents are regarded as a promising technology for CO_2 recovery [7-14]. The dry CO_2 capture process has the following advantages: it is compact, does not discharge wastewater, and is anti-corrosive without requiring an aqueous working solution [15]. Park et al. proposed a novel multi-stage CO_2 capture process that incorporates heat-exchangeable fluidized-bed reactors as a new method for post-combustion CO_2 capture. This multi-stage CO_2 capture technology reduces the energy consumption needed for CO_2 capture from flue gas in post-combustion by using solid sorbents [15-17]. This process requires different types of sorbents for CO_2 capture at low, intermediate, and high temperatures. To date, K_2CO_3-, MgO-, and Li_4SiO_4-based dry regenerable sorbents have been considered for the low- (30-250 °C), intermediate- (250-450 °C), and high- (550-750 °C) temperature stages, respectively [15-17]. In this study, we focus on developing dry sorbents for CO_2 capture at intermediate temperatures.

Many studies have reported MgO-based dry sorbents for CO_2 capture at intermediate temperature because their CO_2 capacity in theory is very high (24.8 mmol/g) [18-24]. One mole of MgO can absorb one mole of CO_2 per the stoichiometry of the following reaction: $MgO+CO_2 \rightleftharpoons MgCO_3$ [25-27]. However, bulk MgO has a very low CO_2 capture capacity of <1 mmol/g due to its slow kinetic reactivity [23,26-30]. The need for higher CO_2 capture capacities is a very important issue.

Mayorga et al. first suggested double-salt sorbents containing magnesium oxide and alkali-metal carbonates and nitrates, which have great potential as sorbents for CO_2 capture at intermediate temperatures [31]. In patent US 6,280,503 B1, it was reported that MgO-based double-salt sorbents showed a maximum CO_2 capture capacity of 12.89 mmol CO_2/g sorbent at 375 °C and 1 atm in the presence of 100 vol% CO_2. In the case of Na-Mg double-salt sorbent, the dried cake is composed of $Mg_5(CO_3)_4(OH)_2{\cdot}4H_2O$, $NaNO_3$, and $Na_2Mg(CO_3)_2$. After activation at 400 °C, the phase components of the double-salt sorbent are MgO, Na_2CO_3, and $NaNO_3$ due to the decomposition of $Mg_5(CO_3)_4(OH)_2{\cdot}4H_2O$ and $Na_2Mg(CO_3)_2$

†To whom correspondence should be addressed.
E-mail: kjchang@knu.ac.kr
‡Soo Chool Lee and Su Ho Cha contributed equally to this work.
‡This article is dedicated to Prof. Seong Ihl Woo on the occasion of his retirement from KAIST.

[25]. Recently, worldwide efforts have attempted to develop alkali-metal nitrate-promoted MgO sorbents for high-capacity pre-combustion CO_2 capture at intermediate temperatures [23-25,30-32]. However, it is difficult to precisely control the amount of alkali-metal nitrate remaining in double-salt absorbents due to the filtration and washing of samples prepared by the precipitation method [25,31]. In addition, the effects of alkali-metal carbonates and nitrates on the CO_2 capture capacities of MgO-based sorbents in the presence of a low concentration of 10 vol% CO_2 for post-combustion CO_2 capture and their regeneration properties have not yet been comprehensively investigated.

In this study, we prepared MgO-based sorbents promoted with various alkali-metal carbonates and nitrates by an impregnation method to mitigate the reproducibility problem of double-salt sorbents. The CO_2 capture capacities of the MgO-based sorbents were investigated in the presence of 10 vol% CO_2 and 10 vol% H_2O in a fixed-bed reactor. In addition, the effects of alkali-metal carbonates and nitrates on the regeneration properties of the sorbents were investigated using temperature-programmed desorption (TPD) analysis.

EXPERIMENTAL

1. Sorbent Preparation

The MgO-based sorbents used in this study were prepared with a typical impregnation method. First, 9.0 g of magnesium oxide (MgO, Aldrich) was added to an aqueous solution containing 1 g of anhydrous alkali-metal nitrates (Aldrich), such as $LiNO_3$, $NaNO_3$, and, KNO_3, in 100 ml of deionized water. For MgO-based sorbents promoted with alkali-metal carbonate, 6.3 g of MgO was added to an aqueous solution containing 2.7 g of anhydrous alkali-metal carbonate (K_2CO_3 and Na_2CO_3, Aldrich) in 90 ml of deionized water. After impregnation, the dried samples were calcined in a furnace under air for 5 h at 500 °C at a ramping rate of 5 °C/min. We denoted these sorbents as ML(N), MN(N), MK(N), MN(C), and MK(C), where M represents MgO; L(N), N(N), and K(N) represent $LiNO_3$, $NaNO_3$, and KNO_3, respectively; and N(C) and K(C) represent Na_2CO_3 and K_2CO_3, respectively. For MgO-based sorbents promoted with both alkali-metal carbonates and nitrates, 9.0 g of the calcined MN(C) or MK(C) sample was added to an aqueous solution containing 1 g of anhydrous alkali-metal nitrates ($LiNO_3$, $NaNO_3$, and KNO_3, Aldrich) in 100 ml of deionized water. After impregnation, the dried samples were calcined under the same conditions as mentioned above. We denoted these sorbents as MN(C)L(N), MN(C)N(N), MN(C)K(N), MK(C)L(N), MK(C)N(N), and MK(C)K(N).

2. CO_2 Sorption Measurement and Characterization

CO_2 sorption and regeneration tests were performed in a fixed-bed quartz reactor (3/4-inch diameter), which was placed in an electric furnace under atmospheric pressure. First, 1 g of the sorbent was packed into the reactor. All volumetric gas flows were measured under standard temperature and pressure (STP). The inlet and outlet lines of the reactor were maintained above 80 °C to prevent condensation of the water vapor being injected into the reactor and GC column. The column used in the analysis was a 1/8-inch stainless tube packed with Porapak Q. CO_2 sorption and regeneration were conducted at 300 °C and 450 °C, respectively, using gas mixtures with the following compositions: (a) 10 vol% CO_2, 10 vol% H_2O, and 80 vol% N_2; and (b) 10 vol% H_2O and 90 vol% N_2, respectively, as shown in Table 1. When the CO_2 concentration of the outlet gases reached that of the inlet gas (10 vol%) in the CO_2 sorption process, nitrogen was introduced for long enough to regenerate the spent sorbents as the CO_2 concentration reached 200 ppm in the multiple-cycle tests. The outlet gases from the reactor were automatically analyzed every minute using a thermal conductivity detector (TCD; Donam Systems Inc., IGC-7200), which was equipped with an auto sampler.

Table 1. Experimental conditions for MgO-based dry sorbents

	CO_2 absorption	Regeneration
Temperature (°C)	300	450
Pressure (atm)	1	1
Flow rate (ml/min)	40	40
Gas composition (vol%)	CO_2: 10, H_2O: 10 N_2: Balance	H_2O: 10 N_2: Balance

Power X-ray diffraction (XRD; Philips, X'PERT Pro MPD-MRD) was also measured to confirm the structure using nickel-filtered CuKα radiation source (λ=0.154 nm) at 40 kV and 25 mA. To identify the regeneration properties, TPD (temperature-programmed desorption) tests of the sorbents were performed under N_2 after CO_2 sorption, when the temperature ramping rate was 1 °C/min.

RESULTS AND DISCUSSION

1. Effects of Alkali-Metal Nitrates on the CO_2 Sorption Properties of MgO-Based Sorbents

Fig. 1 shows the CO_2 capture capacities of a MgO sorbent and MgO-base sorbents promoted with alkali-metal nitrates as a function of time in the presence of 10 vol% CO_2 and 10 vol% H_2O at

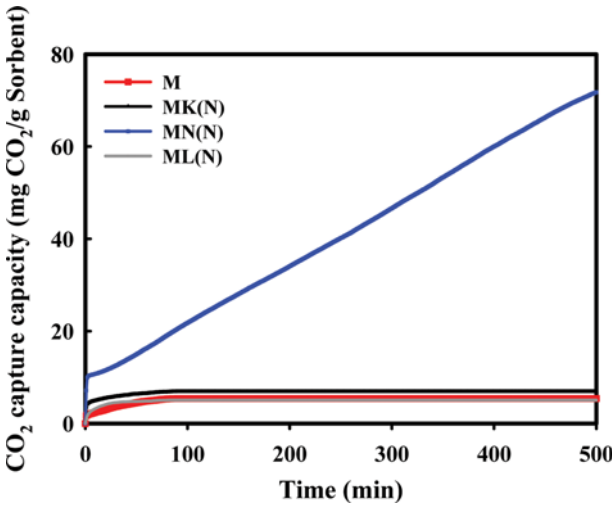

Fig. 1. CO_2 capture capacities of a MgO sorbent and MgO-based sorbents promoted with alkali-metal nitrates as a function of time in the presence of 10 vol% CO_2 and 10 vol% H_2O at 300 °C.

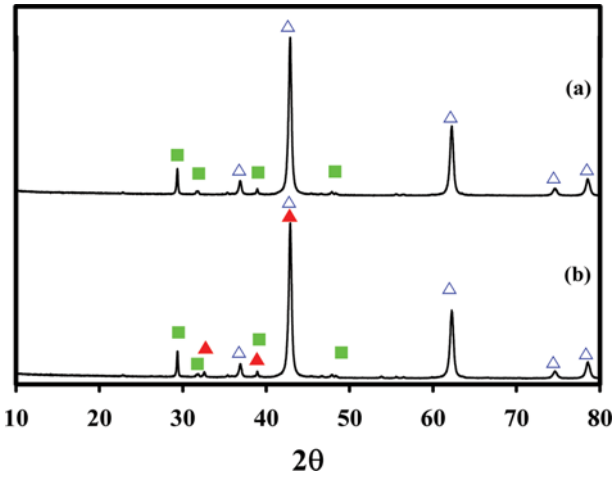

Fig. 2. XRD patterns of the MgO-based sorbents promoted with $NaNO_3$ (a) before and (b) after CO_2 sorption: (△) MgO; (▲) $MgCO_3$; (■) $NaNO_3$.

300 °C. The MgO-base sorbents promoted with alkali-metal nitrates were prepared by the impregnation of MgO with 10 wt% $LiNO_3$, $NaNO_3$, or KNO_3 (ML(N), MN(N), or MK(N), respectively). The Y-axis indicates the CO_2 capture capacity, which was calculated by using a breakthrough curve. As shown in Fig. 1, the MN(N) sorbent promoted with $NaNO_3$ has a relatively high CO_2 capture capacity of 73.2 mg CO_2/g sorbent, even at the low concentration of 10 vol% CO_2, unlike the MgO sorbent and the ML(N) and MK(N) sorbents promoted with $LiNO_3$ and KNO_3, respectively. $NaNO_3$ plays an important role in increasing the CO_2 capture capacity of the MgO-based sorbent in the presence of a low concentration of 10 vol% CO_2 at 300 °C. However, this value was recorded for 500 min, indicating that the sorption rate of the MgO-based sorbent promoted with $NaNO_3$ is very slow at the low concentration of 10 vol% CO_2.

Fig. 2 shows the XRD patterns of the MgO-based sorbents promoted with $NaNO_3$ before and after CO_2 sorption. The XRD pattern of the fresh MN(N) sorbent indicates the presence of MgO (JCPDS No. 87-0651) and $NaNO_3$ phases (JCPDS No. 79-2056). After CO_2 sorption at 300 °C, the XRD patterns of the MN(N) sorbent include three phases, MgO, $MgCO_3$ (JCPDS No. 71-1534), and $NaNO_3$, indicating that the MgO phase is converted into a $MgCO_3$ phase during CO_2 sorption as the following reaction: $MgO + CO_2 \rightleftharpoons MgCO_3$.

2. Effects of Alkali-Metal Carbonates on the CO_2 Sorption Properties of MgO-based Sorbents

To improve the very slow sorption rate of the MN(N) sorbent, we prepared MgO-based sorbents promoted with both alkali-metal carbonates and nitrates by an impregnation method. Fig. 3 shows the CO_2 capture capacities of the MgO-based sorbents promoted with Na_2CO_3 or both Na_2CO_3 and alkali-metal nitrates during multiple cycles as well as the CO_2 capture capacity as a function of time over a single cycle in the presence of 10 vol% CO_2 and 10 vol% H_2O. CO_2 sorption and regeneration were conducted at 300 and 450 °C, respectively. The MN(C) sorbent, which was prepared by impregnating MgO with Na_2CO_3, exhibits a very low CO_2 capture

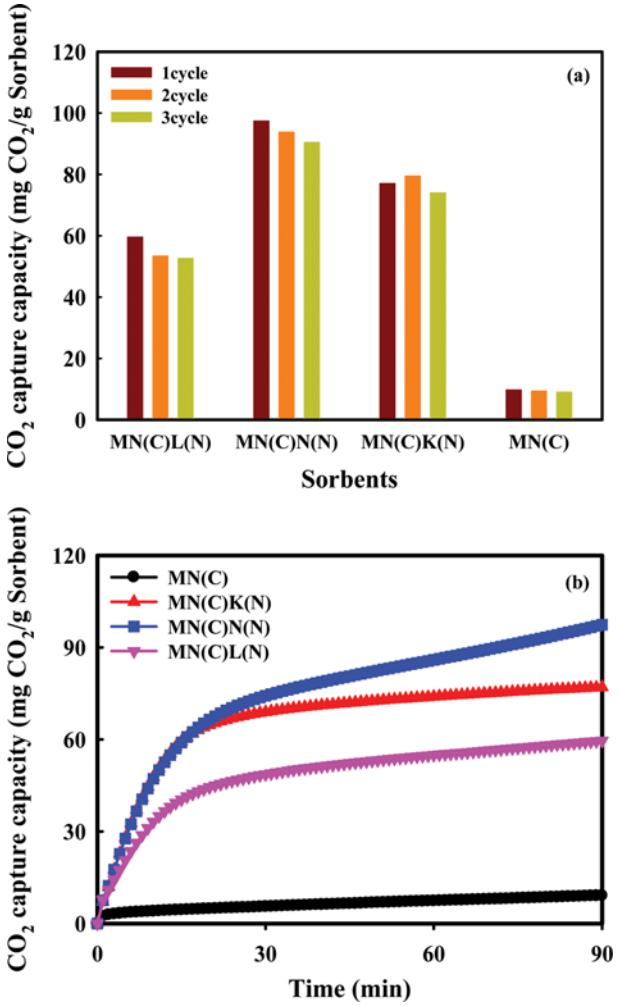

Fig. 3. (a) CO_2 capture capacities of the MgO-based sorbents promoted with Na_2CO_3 or both Na_2CO_3 and alkali-metal nitrates during multiple cycles and (b) CO_2 capture capacity as a function of time over one cycle in the presence of 10 vol% CO_2 and 10 vol% H_2O.

capacity of 9.7 mg CO_2/g sorbent. On the other hand, the CO_2 capture capacities of MgO-based sorbents promoted with both Na_2CO_3 and the alkali-metal nitrates, $LiNO_3$, $NaNO_3$, and KNO_3 (MN(C)L(N), MN(C)N(N), and MN(C)K(N), respectively), are 59.6, 97.4, and 77.0 mg CO_2/g sorbent, respectively, at first cycle. This result indicates that the alkali-metal nitrates play an important role in the CO_2 capture capacity of MgO-based sorbents because of the effect of the molten salt, which removes the high lattice energy constraints of MgO [32,33]. Zhang et al. reported that $[Mg^{2+}\cdots O^{2-}]$ ionic pairs formed by dissolution in molten salt during CO_2 sorption have much weaker interactions than the strong Mg-O ionic bonds in bulk MgO, restricting a direct reaction between MgO and CO_2 [32,33]. Note that in Fig. 3(b) the improvement of the CO_2 sorption rate of the sorbents induced by the addition of Na_2CO_3 to MgO-based sorbents promoted with alkali-metal nitrates is greater than that induced by the MN(N) sorbent promoted with $NaNO_3$. In addition, the reproducibility problem observed for double-salt sorbents prepared by the precipitation method could be

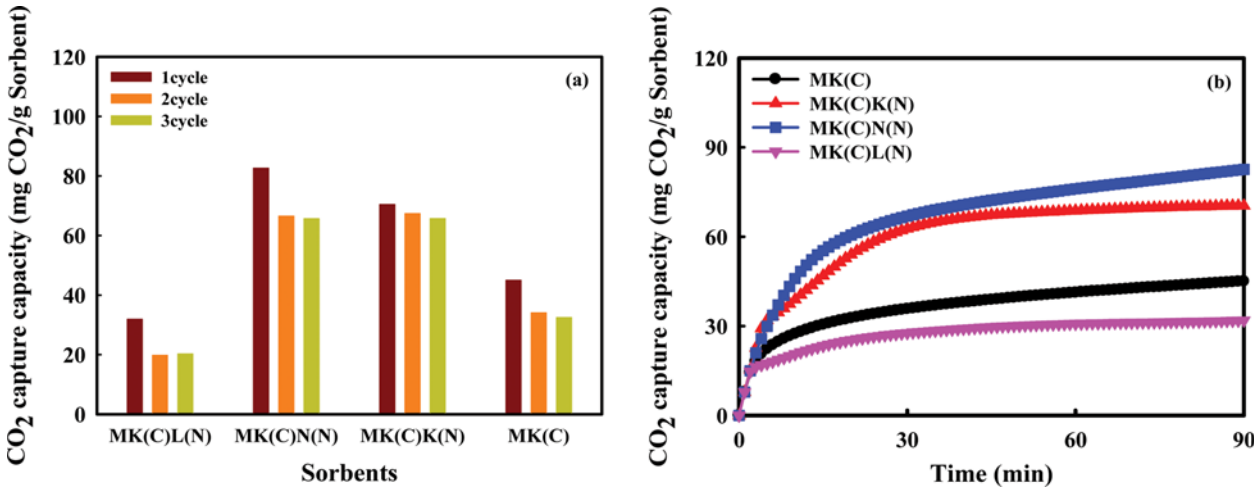

Fig. 4. (a) CO_2 capture capacities of the MgO-based sorbents promoted with K_2CO_3 and both K_2CO_3 and alkali-metal nitrates during multiple cycles and (b) CO_2 capture capacity as a function of time over one cycle in the presence of 10 vol% CO_2 and 10 vol% H_2O.

completely resolved by impregnating MgO with alkali-metal carbonates and nitrates. For the double-salt sorbents reported previously, it is very difficult to control the amount of alkali-metal carbonate and nitrate retained because of the filtering step in double-salt syntheses conducted using the precipitation method [25].

Fig. 4 shows the CO_2 capture capacities of the MgO-based sorbents promoted with K_2CO_3 and both K_2CO_3 and alkali-metal nitrates during multiple cycles as well as the CO_2 capture capacity as a function of time over a single cycle in the presence of 10 vol% CO_2 and 10 vol% H_2O. The MK(C) sorbent promoted with K_2CO_3 without alkali-metal nitrates exhibits a CO_2 capture capacity of 45.0 mg CO_2/g sorbent, which is higher than that of the MN(C) sorbent promoted with a Na_2CO_3. The MK(C)L(N), MK(C)N(N), and MK(C)K(N) sorbents promoted with both K_2CO_3 and an alkali-metal nitrate, namely, $LiNO_3$, $NaNO_3$, or KNO_3, show CO_2 capture capacities of 31.9, 82.4, and 70.2 mg CO_2/g sorbent, respectively. It is thought that the different effects of the alkali-metal nitrates on the CO_2 capture capacities of the sorbents are due to the melting temperatures of the nitrates dispersed on the MgO surface and the CO_2 solubility in the molten salts [25,30-34]. Not only the CO_2

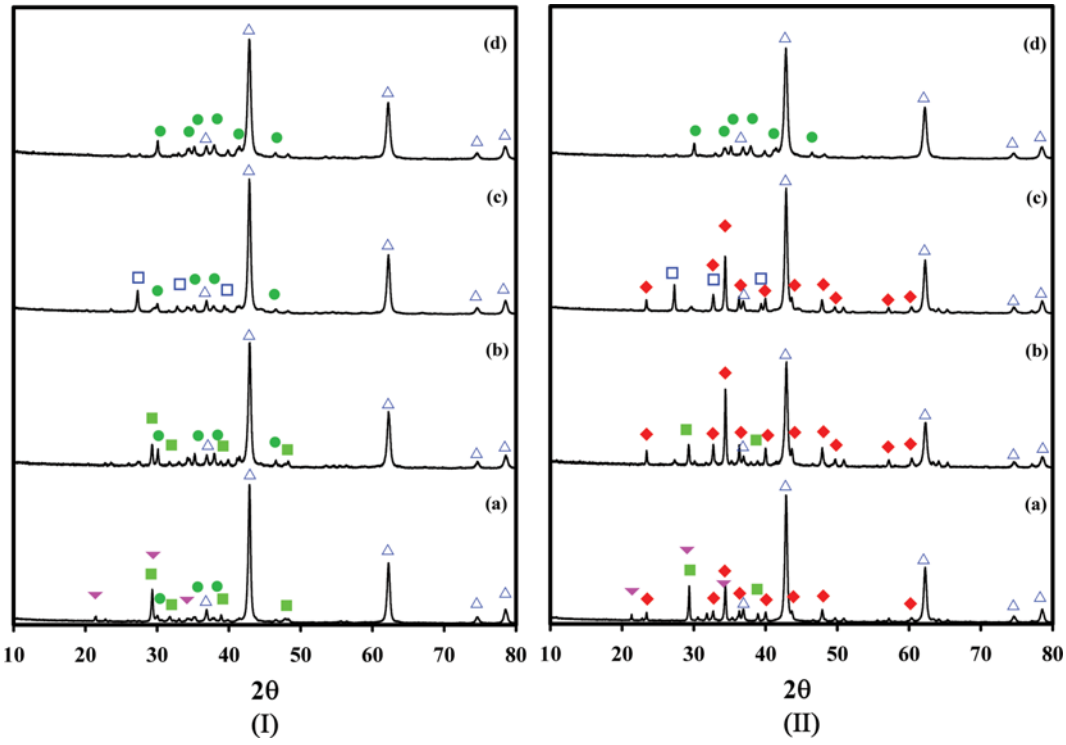

Fig. 5. XRD patterns of the (a) MN(C)L(N), (b) MN(C)N(N), (c) MN(C)K(N), and (d) MN(C) sorbents (I) before and (II) after CO_2 sorption: (△) MgO; (■) $NaNO_3$; (□) KNO_3; (●) Na_2CO_3; (▼) $LiNaNO_3$; (◆) $Na_2Mg(CO_3)_2$.

Table 2. X-ray diffraction patterns of the MgO-based sorbents before and after CO_2 sorption as summarized from XRD analysis

Sorbent	XRD patterns		Sorbent	XRD patterns	
	Fresh	After CO_2 sorption		Fresh	After CO_2 sorption
MN(C)L(N)	MgO, Na_2CO_3 $LiNaNO_3$, $NaNO_3$	MgO, $LiNaNO_3$, $NaNO_3$, $Na_2Mg(CO_3)_2$	MK(C)L(N)	MgO, K_2CO_3 $LiKNO_3$, KNO_3	MgO, $LiKNO_3$, KNO_3, $K_2Mg(CO_3)_2$
MN(C)N(N)	MgO, Na_2CO_3, $NaNO_3$	MgO, $NaNO_3$, $Na_2Mg(CO_3)_2$	MK(C)N(N)	MgO, K_2CO_3, $NaNO_3$, KNO_3	MgO, $NaNO_3$, KNO_3 $K_2Mg(CO_3)_2$
MN(C)K(N)	MgO, Na_2CO_3, KNO_3	MgO, KNO_3, $Na_2Mg(CO_3)_2$	MK(C)K(N)	MgO, K_2CO_3, KNO_3	MgO, KNO_3, $K_2Mg(CO_3)_2$
MN(C)	MgO, Na_2CO_3	MgO, Na_2CO_3	MK(C)	MgO, K_2CO_3	MgO, K_2CO_3 $K_2Mg(CO_3)_2$

capture capacity but also the CO_2 sorption rate of the MK(C)N(N) sorbent could be enhanced by adding K_2CO_3 to the MgO-based sorbents promoted with Na_2NO_3, as shown in Fig. 4(b), indicating that the presence of alkali-metal carbonates is directly related to the CO_2 sorption rate of the MgO-based sorbent. Comparing the CO_2 capture capacities and sorption rates of the MgO-based sorbents shown in Figs. 1, 3, and 4, the MN(C)N(N) sorbent promoted with both Na_2CO_3 and $NaNO_3$ has the best CO_2 sorption properties for the flue gas compositions relevant to post-combustion CO_2 capture. Furthermore, these results indicate that the alkali-metal carbonate must be always added together with Na_2NO_3 to improve the CO_2 capture capacity and sorption rate in the presence of a low CO_2 concentration.

3. Structure Identification of MgO-based Sorbents

The structural changes of the sorbents after CO_2 sorption were examined by XRD. These results are shown in Fig. 5 and 6 and their XRD patterns are summarized in Table 2. Fig. 5 shows the XRD patterns of the MN(C)L(N), MN(C)N(N), MN(C)K(N), and MN(C) sorbents before and after CO_2 sorption. The XRD patterns of the fresh MN(C) sorbent reveal Na_2CO_3 (JCPDS No. 18-1208) and MgO (JCPDS No. 87-0651) phases. The XRD patterns of the fresh MN(C)L(N) sorbent show four phases: $NaNO_3$ (JCPDS No.

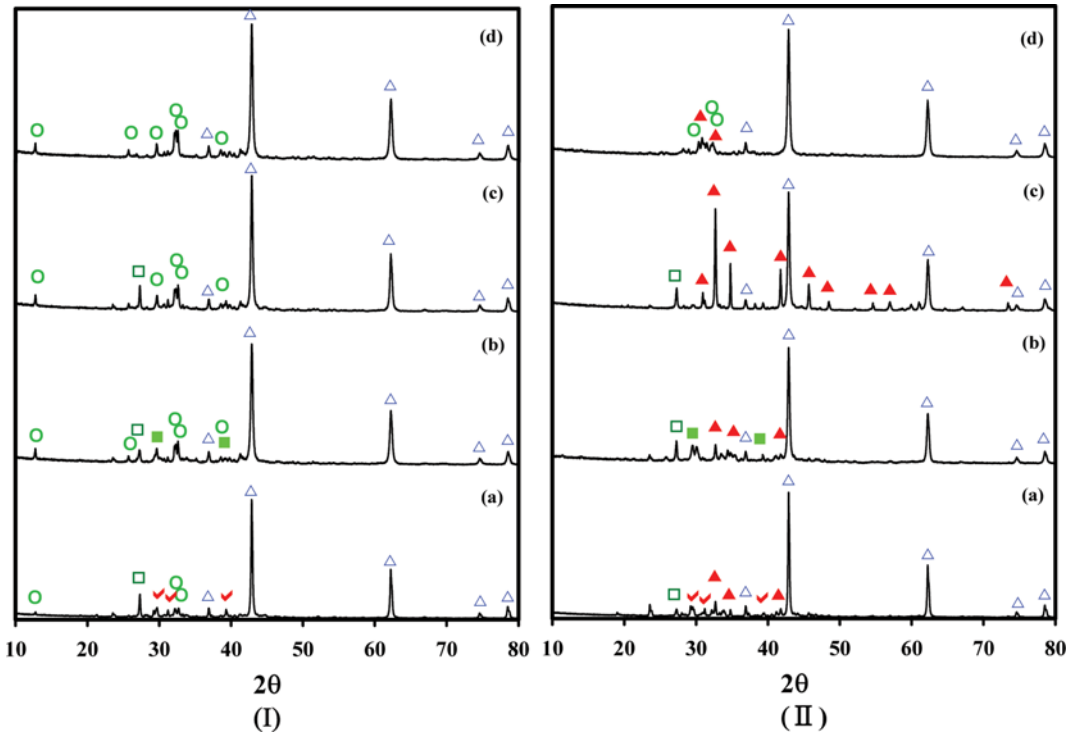

Fig. 6. XRD patterns of the (a) MK(C)L(N), (b) MK(C)N(N), (c) MK(C)K(N), and (d) MK(C) sorbents (I) before and (II) after CO_2 sorption: (△) MgO; (■) $NaNO_3$; (□) KNO_3; (○) K_2CO_3; (√) $LiKNO_3$; (▲) $K_2Mg(CO_3)_2$.

79-2056), $LiNaNO_3$ (JCPDS No. 34-0933), Na_2CO_3, and MgO phases, as shown in Fig. 5(I-a). In these XRD patterns, whereas the $NaNO_3$ and $LiNaCO_3$ phases are observed, the $LiNO_3$ phase is not; this is due to the ion exchange by eutectic reaction of $LiNO_3$ and Na_2CO_3. Based on these results, the CO_2 capture capacity (59.6 mg CO_2/g sorbent) of the MN(C)L(N) sorbent is higher than those of the MN(C) and ML(N) sorbents (9.7 and 5.4 mg CO_2/g sorbent, respectively) because of the effect of the $NaNO_3$ produced by ion exchange between $LiNO_3$ and Na_2CO_3. The XRD patterns of the fresh MN(C)N(N) and MN(C)K(N) sorbents show three phases, $NaNO_3$ and KNO_3 (JCPDS No. 76-1693), respectively, in addition to the Na_2CO_3 and MgO phases. All the XRD patterns of the MN(C)L(N), MN(C)N(N), and MN(C)K(N) sorbents after CO_2 absorption include a $Na_2Mg(CO_3)_2$ phase (JCPDS No. 71-0933), which results from the reaction of Na_2CO_3 and MgO with CO_2 according to the CO_2 sorption mechanism, $Na_2CO_3+MgO+CO_2 \rightleftharpoons Na_2Mg(CO_3)_2$ [24,25,33].

Fig. 6 shows the XRD patterns of the MK(C)L(N), MK(C)N(N), MK(C)K(N), and MK(C) sorbents before and after CO_2 sorption. The XRD pattern of the fresh MK(C) sorbent reveals K_2CO_3 and MgO phases. For the MK(C)L(N) sorbent, new $LiKCO_3$ (JCPDS No. 88-0341) and KNO_3 phases without $LiNO_3$ are observed in addition to the K_2CO_3 and MgO phases, as shown in Fig. 6(I-a). In the case of the MK(C)N(N) sorbent, new KNO_3 phase is observed in addition to $NaNO_3$, K_2CO_3, and MgO phases, as shown in Fig. 6(b). These results obtained from the XRD patterns of Fig. 6(I-a and b) are attributed to the ion exchange resulting from the eutectic reaction between $LiNO_3$ or $NaNO_3$ and K_2CO_3, as mentioned above. On the other hand, the XRD patterns of the MK(C)K(N) sorbent show three phases, KNO_3, K_2CO_3, and MgO. After CO_2 sorption, as evident in all the XRD patterns in Fig. 6(II) and Table 2, a $K_2Mg(CO_3)_2$ phase (JCPDS No. 75-1725) is observed.

4. Effects of Temperature on the CO_2 Capture Capacity of MgO-based Sorbents

Fig. 7 shows the CO_2 capture capacities of the MN(C)N(N), MN(C)K(N), MK(C)N(N), and MK(C)K(N) sorbents as a function of temperature. The CO_2 capture capacity of all these sorbents was highest at 300 °C. The CO_2 capture capacities of the MN(C)N(N), MN(C)K(N), MK(C)N(N), and MK(C)K(N) sorbents rapidly decreased as the temperature further increased to 350 °C. The MK(C)N(N) sorbent includes a $NaNO_3$-KNO_3 binary mixture (MP: 221 °C), which has a melting temperature much lower than that of $NaNO_3$ (MP: 308 °C) or KNO_3 (MP: 329 °C) alone [32-34]. Nevertheless, the CO_2 capture capacity of the MK(C)N(N) sorbent at 250 °C was lower than that at 300 °C. Meanwhile, interestingly, at 250 °C, the CO_2 capture capacity of the MN(C)N(N) sorbent is higher than those of other sorbents and is similar to its value at 300 °C.

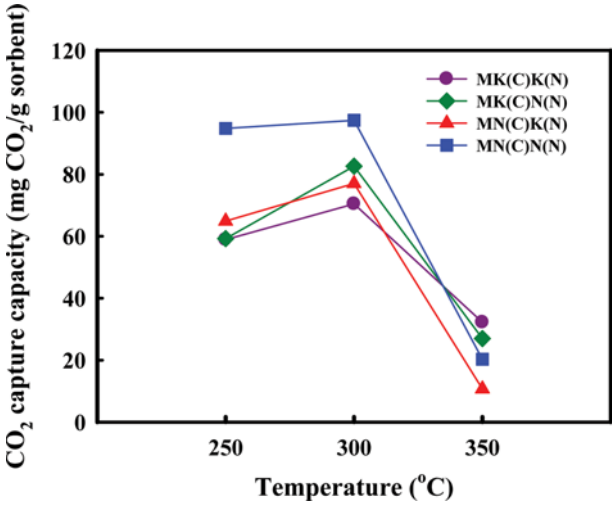

Fig. 7. CO_2 capture capacities of the MN(C)N(N), MN(C)K(N), MK(C)N(N), and MK(C)K(N) sorbents as a function of temperature.

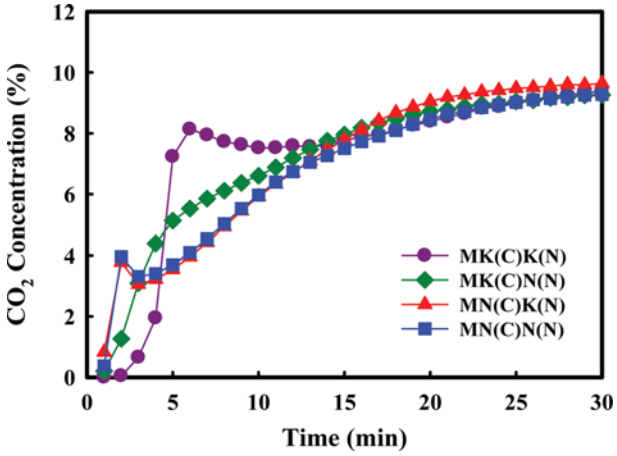

Fig. 8. CO_2 breakthrough curves of the MK(C)N(N), MK(C)K(N), MN(C)N(N), and MN(C)K(N) sorbents in the presence of 10 vol% CO_2 and 10 vol% H_2O at 300 °C.

Fig. 8 shows the CO_2 breakthrough curves of the MK(C)N(N), MK(C)K(N), MN(C)N(N), and MN(C)K(N) sorbents in the presence of 10 vol% CO_2 and 10 vol% H_2O at 300 °C. Two-step CO_2 sorption behavior was observed in the breakthrough curves of the MK(C)K(N), MN(C)N(N), and MN(C)K(N) sorbents. First, alkali-metal-Mg double-salt is formed by initial CO_2 sorption at 300 °C. The eutectic reaction is then accelerated via an exothermic carbonation reaction during the initial CO_2 sorption. Second, new MgO active sites, which are produced through the formation of the Na-Mg or K-Mg double-salt and the eutectic reaction, react slowly with K_2CO_3 and CO_2. These results indicate that an activation process via the eutectic reaction of alkali-metal nitrates is crucial for the sorption of CO_2 over MgO-based sorbents. In the MK(C)N(N) sorbent, however, a typical breakthrough curve is observed, resulting from a rapid eutectic reaction at a lower melting temperature (MP: 221 °C) contributed by the binary mixture of the $NaNO_3$-KNO_3 produced by ion exchange between K_2CO_3 and $NaNO_3$.

5. Regeneration Properties of MgO-based Sorbents

Fig. 9 shows the TPD results for Mg-based sorbents after CO_2 sorption at 300 °C. These results were obtained by measuring the concentration of CO_2 desorbed when the temperature ramping rate was 1 °C/min. For the MK(C) sorbent, the highest CO_2 peak is observed at 400 °C, which is almost consistent with the peak

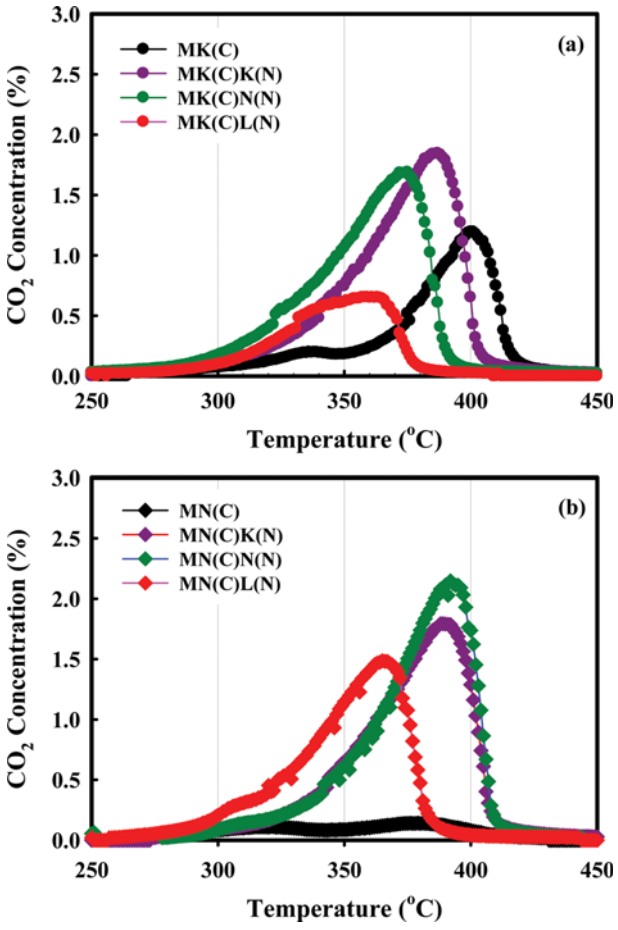

Fig. 9. TPD results for Mg-based sorbents after CO_2 sorption at 300 °C.

location of $K_2Mg(CO_3)_2$. On the other hand, the highest CO_2 peaks of the MgO-based sorbents promoted with both alkali-metal carbonate and nitrate are found at lower temperatures than the highest peak of the MK(C) sorbent. In particular, the highest peaks of the MN(C)L(N), MK(C)L(N), and MK(C)N(N) sorbents with two types of alkali-metal nitrates, which were produced by a eutectic reaction between alkali-metal carbonates and nitrates, are observed at lower temperatures than those of other sorbents. These results indicate that the regeneration temperature of MgO-based sorbents can be reduced by promotion with alkali-metal nitrates due to the effect of the molten salt. To identify the effect of alkali-metal nitrates on the regeneration temperature of the MgO-based sorbent, alkali-metal nitrates were added by physical mixing after a MgO-based sorbent promoted with K_2CO_3 (MK(C)) had been used for CO_2 sorption. TPD tests of these samples were conducted under the same conditions. As shown in Fig. 10, the regeneration temperatures of the MgO-based sorbents containing alkali-metal nitrates are lower than that of the MK(C) sorbent without alkali-metal nitrates. It is clear that the regeneration properties of the MgO-based sorbent are affected by the alkali-metal nitrates because of the molten salt effect during the regeneration process. From these results, we conclude that the molten alkali-metal nitrate plays an important role in the sorption and regeneration properties of the

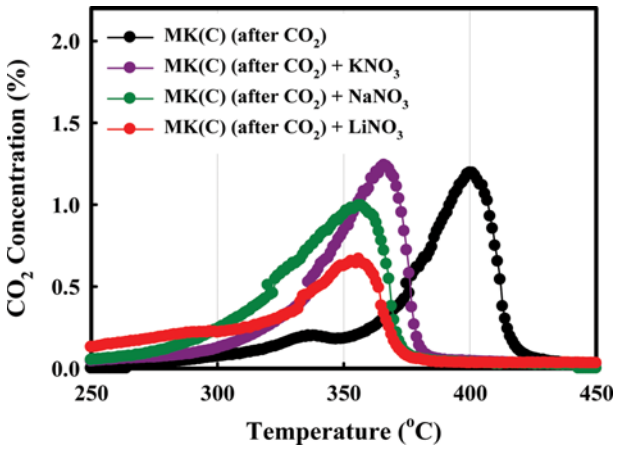

Fig. 10. TPD results for the MK(C) sorbent and materials prepared by physical mixing of the MK(C) sorbent after CO_2 sorption with $LiNO_3$, $NaNO_3$, or KNO_3.

MgO-based sorbent.

CONCLUSIONS

MgO-based sorbents promoted with alkali-metal carbonates and nitrates were prepared by impregnating MgO with alkali-metal carbonates and nitrates. The reproducibility problem of double-salt sorbents caused by their preparation by the precipitation method was completely resolved by the use of the impregnation method. A MgO-based sorbent promoted with both Na_2CO_3 and $NaNO_3$ exhibited a high CO_2 capture capacity of 97.4 mg CO_2/g sorbent, even at a low concentration of 10 vol% CO_2 at 300 °C, demonstrating that its CO_2 sorption rate is higher than those of the MgO-based sorbents promoted with alkali-metal nitrates. In particular, their desorption temperatures are lower than those of the MgO-based sorbents promoted with alkali-metal carbonates, which results from a eutectic reaction during the regeneration process.

ACKNOWLEDGEMENTS

We acknowledge the financial support by grants from Korea CCS R&D Center, funded by the Ministry of Education, Science and Technology of Korean government (NRF-2014M1A8A1049249). This work was supported by the Human Resources Program in Energy Technology of the Korea Institute of Energy Technology Evaluation and Planning (KETEP), granted financial resource from the Ministry of Trade, Industry & Energy, Republic of Korea (no. 20144010200670).

REFERENCES

1. Intergovernmental Panel on Climate Chang (IPCC) (2005) IPCC special report on carbon dioxide capture and storage, http://www.ipcc.ch.
2. H. Herzog, in *Carbon dioxide capture and storage*, D. Helm and C. Hepburn Eds., Oxford U. Press (2009).
3. T. H. Oh, *Renew. Sust. Energy Rev.*, **14**, 2697 (2010).

4. K.-C. Kim, Y. C. Park, S.-H. Jo and C.-K. Yi, *Korean J. Chem. Eng.*, **28**(10), 1986 (2011).
5. K. S. Kim, S. R. Yang, J. B. Lee, T. H. Eom, C. K. Ryu, H.-J. Lee, T.-S. Bae, Y.-B. Lee and S.-J. Lee, *Korean J. Chem. Eng.*, **32**(4), 677 (2015).
6. Y. C. Park, S.-H. Jo, C. K. Ryu and C.-K. Yi, *Energy Procedia*, **1**(1), 1235 (2009).
7. Y. C. Park, S.-H. Jo, S.-Y. Lee, J.-H. Moon, C. K. Ryu, J. B. Lee and C.-K. Yi, *Korean J. Chem. Eng.*, **33**(1), 73 (2016).
8. S. C. Lee, H. J. Chae, S. J. Lee, B. Y. Choi, C. K. Yi, J. B. Lee, C. K. Ryu and J. C. Kim, *Environ. Sci. Technol.*, **42**(8), 2736 (2008).
9. B. Arias, G. Grasa, M. Alonso and J. C. Abanades, *Energy Environ. Sci.*, **5**(6), 7353 (2012).
10. S. Cui, W. Cheng, X. Shen, M. Fan, A. Russell, Z. Wu and X. Yi, *Energy Environ. Sci.*, **4**, 2070 (2011).
11. S. C. Kwon, M. Fan, H. F. M. Dacosta, A. G. Russell and C. Tsouris. *J. Phys. Chem. A*, **115**(26), 7638 (2011).
12. K. W. Kim, Y.-K. Park, J. H. Park, E. J. Jung, H. M. Seo, H. Y. Kim and K. S. Lee, *Energy Procedia*, **63**, 1151 (2014).
13. S. C. Lee, B. Y. Choi, T. J. Lee, C. K. Ryu, Y. S. Ahn and J. C. Kim, *Catal. Today*, **111**, 385 (2006).
14. S. C. Lee, H. J. Chae, B. Y. Choi, S. Y. Jung, C. Y. Ryu, J. J. Park and J. C. Kim, *Korean J. Chem. Eng.*, **28**(2), 480 (2011).
15. H. K. Moon, H. J. Yoo, H. W. Seo, Y.-K. Park and H. H. Cho, *Energy*, **84**, 704 (2015).
16. K. W. Kim, D. W. Kim, Y.-K. Park and K. S. Lee, *Int. J. Greenhouse Gas Control*, **26**, 135 (2014).
17. Y.-K. Park, H. M. Seo, W. C. Choi, N. Y. Kang, S. Y. Park, D. Y. Min, K. W. Kim, K. S. Lee, H. K. Moon, H. H. Cho and D. K. Lee, *Energy Procedia*, **63**, 2266 (2014).
18. A. Hassanzadeh and J. Abbasian, *Fuel*, **89**(6), 1287 (2010).
19. S.-Y. Lee and S.-L. Park, *J. Ind. Eng. Chem.*, **23**, 1 (2015).
20. G. Xiao, R. Singh, A. Chaffee and P. Webley, *Int. J. Greenhouse Gas Control*, **5**, 634 (2011).
21. S. Wang, S. Yan, X. Ma and J. Gong, *Energy Environ. Sci.*, **4**, 3805 (2011).
22. A. T. Vu, Y. Park, P. R. Jeon and C. H. Lee, *Chem. Eng. J.*, **258**, 254, (2014).
23. X. Yang, L. Zhao and Y. Xiao, *Energy Fuels*, **27**(12), 7645 (2013).
24. C. H. Lee, S. Y. Mun and K. B Lee, *Chem. Eng. J.*, **258**, 367 (2014).
25. K. Zhang, X. S. Li, Y. Duan, D. L. King, P. Singh and L. Li, *Int. J. Greenhouse Gas Control*, **12**, 351 (2013).
26. J. Fagerlund, J. Highfield and R. Zevenhoven, *RSC Adv.*, **2**, 10380 (2012).
27. S. J. Gregg and J. D. Ramsay, *J. Chem. Soc. A*, 2784 (1970).
28. D. Beruto, R. Botter and A. W. Searcy, *J. Phys. Chem.*, **91**, 3578 (1987).
29. R. Philipp and K. Fujimoto, *J. Phys. Chem.*, **96**, 9035 (1992).
30. T. Harada and T. A. Hatton, *Chem. Mater.*, **27**(23), 8153 (2015).
31. S. G. Mayorga, S. J. Weigel, T. R. Gaffney and J. R. Brzozowski, US 6,280,503 B1 (2001).
32. K. Zhang, X. S. Li, W. Z. Li and A. Rohatgi, *Adv. Mater. Interfaces*, **1(3)**, 1400030 (2014).
33. K. Zhang, X. S. Li, H. Chen, P. Singh and D. L. King, *J. Phys. Chem. C*, **120**(2), 1089 (2016).
34. T. Harada, F. Simeon, E. Z. Hamad and T. A. Hatton, *Chem. Mater.*, **27**(6), 1943 (2015).
35. Y. Duan, K. Zhang, X. S. Li, D. L. King, B. Li, L. Zhao and Y. Xiao, *Aerosol Air Qual. Res.*, **14**, 470 (2014).